On Forecasts of the COVID-19 Pandemic

T. J. Mazurek

t_j_mazurek@yahoo.com

Revised: January 8, 2021 Posted: November 11, 2020

Abstract

The current COVID-19 pandemic creates seemingly chaotic devastations. Scientists worldwide have failed to predict actual outcomes. A comprehensive study by (Ioannidis, et.al. 2020) examines detailed reasons for the failures. A second study (Taleb, et.al 2020) questions the approaches used for pandemic prediction. They find that the pandemic distribution has a fat tail, and proclaim this result has significant implication for pandemic predictions. The latter study used the Generalized Pareto Distribution. This study examines the historical pandemic series using the truncated Pareto I distribution. It uses the least-squares-fit estimate for this distribution to determine a precise estimate of the tail exponent 1.15. This study uses Monte Carlo techniques to generate synthetic power law series with this exponent. Applying extreme value theory, it compares the characteristics of the pandemic series to that of power law synthetics. The comparisons show excellent agreement between the historical pandemic series and the synthetic ones. This shows that the pandemic's distribution behaves like the synthetics with this power law, confirming that this distribution is likely to have a fat tail. This study then examines the worldwide countries' mortality rates in ways similar to those used for the historical pandemic. It finds that this distribution may also have a fat tail with a tail exponent of 1.45. This work notes that the historical pandemic distribution is fixed, while it shows that the distribution of the mortality rates continually evolves. The pandemic and mortality distributions' power law behaviors red-light their high danger, demanding extreme caution for dealing with plagues. However, the fat-tailed distributions cannot make specific predictions. Improved forecasts like those championed by (Ioannidis, et.al. 2020) may provide useful guidance for and aid in monitoring the worldwide countries' individual pandemic responses.

1. Introduction

The current COVID-19 pandemic engulfing the world creates wide spread devastations that seemingly are unpredictable. Although many esteemed scientists worldwide have expended great efforts to forecast epidemic courses for individual countries and cities, their forecasts have differed markedly from actual outcomes. A comprehensive study (Ioannidis, Cripps, and Tanner 2020) examines in great detail the reasons for the forecasting failures.

A significant paper by Taleb, Bar-Yam, and Cirillo (2020) questions the approaches used for pandemic prediction by the worldwide researchers, and claims that they are fundamentally flawed. Examining historical pandemics that claimed at least 1000 lives, they find the pandemics' distribution has a fat tail. They proclaim that the presence of fat tails demands profound changes in forecasting pandemic risks. They suggest several modifications to the approach and focus of forecasting. Let's now highlight their salient points.

Fat-tailed distributions have very large (or infinite) means that lie far above the values of the most frequently occurring events. Hence studies of the latter events comprise wasted efforts for risk implications. These frequent occurrences are like noise when compared to the much greater risks residing in the tails.

While random variable distributions with fat tails have unstable (divergent) moments, they may still have stable and informative tail properties for inferences on risk. Hence one should not stall and demand more data since the data to come will still be of the most frequently occurring type, i.e., noise compared to the risk in the tails. Sufficient evidence of huge tail risk is contained in the tail properties themselves.

Forecasting about the mean (or other parameters) of a phenomenon requires that the phenomenon's distribution permits convergences. Extreme value theory shows that relevant distributions for pandemics have divergent means. Thus, extreme value theory should be applied to tail behavior to assess the risk posed by pandemics. Hence in their view, the worldwide forecaster's focuses are "extremely misplaced".

(Ioannidis et.al. 2020) --who's primary focus is on their extensive and detailed examination of reasons behind forecasting failures-- question the above characterization and make several responses, seeking further clarification from (Taleb et.al. 2020). The present study addresses one of their queries, where they posit that a "two parameter Gamma distribution fitted to log counts" may adequately explain the historical pandemic data. This study addresses whether or not Gamma functions can represent the pandemic data. It will examine two Gamma function fits: 1) where its arguments are the pandemic data, and 2) where they are the logarithms of the data (as posited by Ioannidis et.al.).

An earlier ground breaking work by Cirillo and Taleb (2020) forms the foundation for the arguments of Taleb et.al. (2020). It applies the Generalized Pareto Distribution[1] to study the historical pandemic series. The present work uses the truncated Pareto I distribution, applying its least-squares-fit estimate to make a precise determination of the power law exponent. This permits detailed comparisons to synthetic power law series generated via Monte Carlo techniques. These comparisons substantially confirm that the historical pandemic series follows a fat-tailed power law as originally deduced by Cirillo and Taleb (2020).

The statistics on Covid-19 worldwide mortality by country are available at the Johns Hopkins Coronavirus Resource Center's web site[2]. In particular the site provides statistics on deaths per 100K population for each country. For simplicity, this work refers to these statistics as mortality rates. The mortality rates in this work were copied from the Resource Center's posting on 8/31/20. This data is in Table A2.1 in Appendix 2. Figure 1.1 shows the mortality rates in decreasing rank order of the series elements.

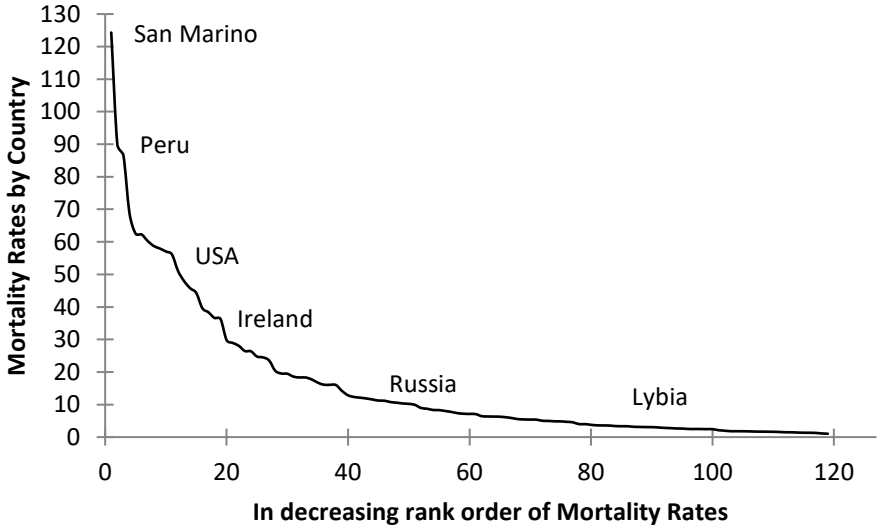

Figure 1.1 Mortality rates by countries in decreasing rank order of mortality rate.

The positions of several countries are labeled on this curve. The plot suggests that the worldwide countries' mortality rates have a fat-tailed distribution. This study examines that possibility and discovers that this is the case. It also finds that this fat-tailed distribution's exponent is evolving noticeably on timescales of roughly weeks.

The remainder of this paper is structured as follows. Section 2 uses the least-squares-fit estimate for the Pareto I distribution to determine the historical pandemic's power law exponent which is $\alpha + 1 = 1.15$. The section applies extreme value theory to study the pandemic distribution. It

[1] See Cirillo (2013) for the various classifications of Pareto distributions.

[2] The statistics are available at: https://coronavirus.jhu.edu/data/mortality .

uses Monte Carlo methods to generate several synthetic series sets corresponding to the historical pandemic one. Using extreme value theory, it then shows that the synthetic series sets have very similar characteristics to that of the historical pandemic one. Section 3 examines the distribution of the world's individual country mortality rates. It finds that the distribution of country morality rates is also fat-tailed. It then examines this distribution in a manner similar to that in Section 2, and finds the mortality rate power law exponent is $\alpha + 1 = 1.45$. The section again uses Monte Carlo methods to generate several synthetic series sets corresponding to the empirical one. It shows that the synthetic series in this set have similar characteristics to that of the empirical mortality rate series. Section 4 presents a summary of the results and discusses implications for pandemic and epidemic forecasting. It also shows the evolutionary behavior of the worldwide mortality rate distribution's power law exponent.

Finally, Appendix 1 determines the maximum likelihood parameters of the Gamma distributions that correspond to the historical pandemic series. This is done for both Gamma function representations of the data as noted above. Using Monto Carlo techniques to generate several sets of deviates for each type of Gamma function fit to the pandemic data, it finds that the both Gamma function distributions have characteristics markedly different from that of the pandemic data, and hence they are not relevant to pandemic studies.

2. Comparing Series: Truncate Pareto I to the Historical Pandemic

The historical pandemic series was copied from Table1 of Cirillo and Taleb (2020). The series is given in that table's column seven, labeled Rescaled Avg Est (×10^3); its elements are in units of 1000. This section uses the truncated Pareto I distribution. It presents the maximum likelihood estimate for this distribution's power law exponent as well as the least-squares-fit estimate of the latter. It finds that the least-squares-fit estimate to be a better representation of the historical pandemic series. The section then presents the mean excess above threshold plot for the pandemic series. It introduces Monte Carlo procedures for generating the synthetic power law series. It generates nine sets of such series and compares characteristics of the historical pandemic to the synthetics. Specifically, the Zipf plots of the pandemic series are shown to be very similar to those of the synthetics. The historical pandemic mean excess behavior with increasing thresholds also essentially matches that of the synthetics. These similarities strongly suggest that the historical pandemic distribution is likely to be a power law with exponent $\alpha + 1 = 1.15$. Finally, it compares the maximum-to-sum plots of one of the synthetics to that of the historical pandemic. The two plots are quite similar, showing that the pandemic distribution mimics the behavior of the fat-tailed power law distributions, so its distribution is also likely to be fat tailed.

The power law distribution used here is the truncated Pareto I distribution (cf. Aban, Meerschaert, Panorska, 2006, equation 3) with exponent $\alpha + 1$, lower bound x_0, and the cut-off x_{max}/x_0:

$$f(x/x_0) = \frac{(\alpha/x_0)(x/x_0)^{-\alpha-1}}{1-(x_0/x_{max})^{\alpha}} \qquad 0 < x_0 \leq x \leq x_{max} < \infty \tag{2.1}$$

Let's set $x_0 = 1000$, the unit used in this section. The cut-off is at the maximum element of the historical pandemic series is $x_{max}/x_0 = 2{,}678{,}283$.

The maximum likelihood α for the truncated Pareto I distribution (cf. ibid, equation 4) satisfies the following two equations

$$\alpha_{mle} = \frac{1}{\left[\frac{1}{n}\sum_{m=1}^{m=n} ln(x_m/x_0) - \eta\right]}, \qquad \eta = \frac{(x_0/x_{max})^{\alpha_{mle}}\, ln(x_0/x_{max})}{1-(x_0/x_{max})^{\alpha_{mle}}}. \tag{2.2}$$

The term $\frac{1}{n}\sum_{m=1}^{m=n} ln(x_m/x_0)$ in the denominator of the first equation is the reciprocal of the maximum likelihood estimate α_∞ for the corresponding unbounded Pareto I distribution ($x_{max} = \infty \rightarrow \eta = 0$). To determine the parameter α_{mle} for the truncated Pareto I distribution, one first determines α_∞. Subsequently one calculates η, then α_{mle}, and continues iterating until the change in α_{mle} per iteration becomes negligible. For the historical pandemic series $\alpha_\infty = 0.15$, resulting in $\alpha_{mle} = 0.0414$.

The truncated Pareto I cumulative distribution (cf. ibid, equation 2) is

$$F(x/x_0) = 1 - \frac{[(x/x_0)^{-\alpha} - (x_{max}/x_0)^{-\alpha}]}{1-(x_{max}/x_0)^{-\alpha}}. \tag{2.3}$$

The least-squares-fit method determines α_{lsf} as follows. Using the empirical logarithmic complementary cumulative distribution $ln[1 - F_{emp}(x/x_0)\,]$, one minimizes the sum of the squared differences between the corresponding empirical and Pareto I logarithmic distributions with respect to α to define α_{lsf}. The pandemic series least-squares-fit result is $\alpha_{lsf} = 0.15$.

Figure 2.1 below shows the double logarithmic plot of the empirical complementary cumulative distribution $ln[1 - F(x/x_0)\,]$ versus $ln(x/x_0)$, i.e., the Zipf plot of the historical pandemic series (dotted points). The figure also shows the corresponding curves for the truncated Pareto I distributions for α_{mle} (dashed line) and α_{lsf} (solid line) along with their R^2 values of 0.72 and 0.94, respectively. The least-squares-fit is clearly a much better representation of the historical pandemic data. The remainder of this section thus sets $\alpha = \alpha_{lsf} = 0.15$ so that the power law exponent is $1 + \alpha = 1.15$. This section uses this power law to compare the historical pandemic series to Monte Carlo synthetic series with equal lengths of 72.

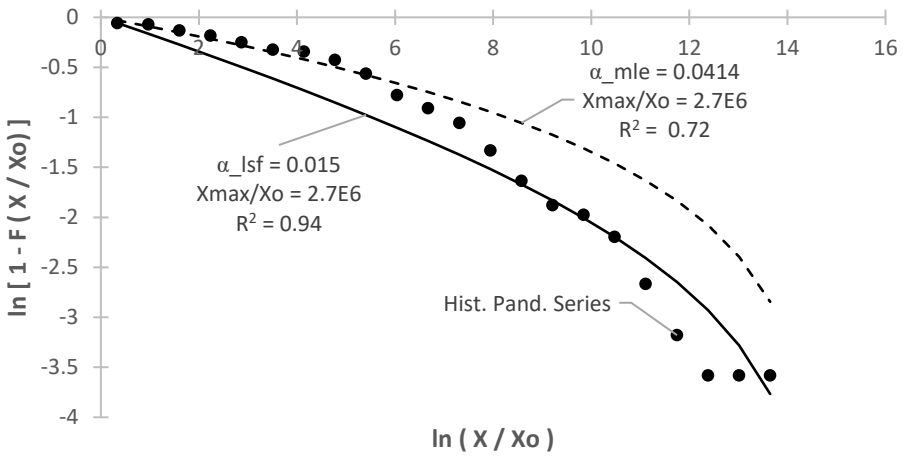

Figure 2.1 Zipf plots of the historical pandemic series, and of the truncated Pareto I distributions with α_{mle} and α_{lsf}.

Let us now consider the empirical mean excess function $e(u/x_0)$ above the threshold u for this distribution which is given by

$$e(u) = E(X-u|X \geq u) = \frac{\int_u^{x_{max}} (x-u)f(x)dx}{\int_u^{x_{max}} f(x)dx} = \frac{\alpha}{1-\alpha} x_{max} \frac{1-\left(\frac{u}{x_{max}}\right)^{1-\alpha}}{\left(\frac{u}{x_{max}}\right)^{-\alpha}-1} - u. \tag{2.4a}$$

Expressed in units of x_0 of this section, one has

$$\frac{e(u)}{x_0} = \left[\frac{\alpha}{1-\alpha}\frac{x_{max}}{x_0}\frac{1-\left(\frac{u}{x_{max}}\right)^{1-\alpha}}{\left(\frac{u}{x_{max}}\right)^{-\alpha}-1} - \frac{u}{x_0}\right]. \tag{2.4b}$$

If a random variable has a fat tail the mean excess should increase with increasing threshold (cf. Embrechts et. al. 2003). For unbounded Pareto I distributions with convergent means ($\alpha > 1$), the mean excesses are linear with slopes equal to $(\alpha-1)^{-1}$. Note the slope of the mean excess curve here at x_0 is huge, $\frac{d}{d\left(\frac{u}{x_0}\right)}\left[\frac{e(u)}{x_0}\right]|_{u=x_0} \cong 10^4$, and it remains of this order of magnitude over an extended range of u/x_0. The slopes of the mean excess here grow much more steeply than those of the overwhelming majority[3] of unbounded and convergent Pareto I distributions, indicating much fatter tails.

The empirical mean excess function $e(u)$ above the threshold u (cf. Embrechts, Klüppelberg and Mikosch, 2003, p. 296, their equation 6.6) is given by

$$e(u)/x_0 = \frac{1}{n_{x_i \geq u}} \sum_{n_{x_i \geq u}} (x_i - u)/x_0. \tag{2.5}$$

[3] Of all these distributions only those with $\alpha = 1+\varepsilon$, where $\varepsilon \ll 1$ have comparable large slopes.

In this equation $n_{x_i \geq u}$ is the total number of series elements satisfying $x_i \geq u$.

Now consider Monte Carlo procedures for generating truncated Pareto I synthetic series of the same length as the historical pandemic one. The formula (cf. Clauset, Shalizi, and Newman, 2009, p. 40) for generating synthetic power law deviates x_k^{syn} with a power law exponent γ is

$$x_k^{syn} = y_0(1 - r_k)^{\frac{-1}{\gamma - 1}}. \tag{2.6}$$

In this formula $r_k \in (0,1)$ is the kth uniformly distributed deviate. To generate the latter deviates, this work uses the ran1 program of Press, Flannery, and Teukolsky (2002, p. 280).

The following procedure generated the synthetic series deviates, setting $y_0 = 1$ and $\gamma = \alpha + 1 = 1.15$ in equation (2.6). The unit used here is 1000, i.e., only pandemics with at least 1000 fatalities are included. The number and distribution of pandemics below this threshold is unknown. Also, one has no knowledge about pandemics above the maximum element x_{max} in the historical pandemic series. Hence one generates a series with the number of deviates n_d where $n_d > 72$. Deviates below 1000 and deviates above x_{max} are discarded. One now selects 72 elements out of the remaining ones, dividing them by 1000 to express them in the units used here. Nine sets of synthetic series each having 72 deviates were generated. Finally, each deviate in all nine sets, is multiplied by the normalizing factor $\alpha/[x_0(1 - (x_0/x_{max})^{\alpha})]$ to obtain the truncated Pareto I distribution deviates.

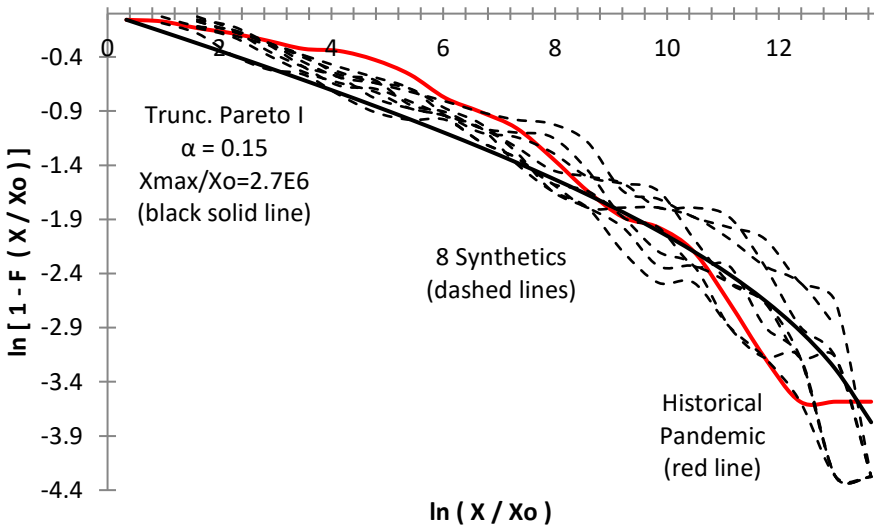

Figure 2.2 Zipf plots for the historical pandemic series, 8 synthetic series, as well as that of the corresponding truncated Pareto I.

Figure 2.2 above shows Zipf plots for the historical pandemic series (red solid line), 8 Monte Carlo synthetic series (dashed lines), as well as that of the corresponding truncated Pareto I of

equation (2.3). One can see that the paths of the synthetic power-law series envelop the path of the historical pandemic series. Thus the historical pandemic series mimics the behavior of the heavy tailed synthetics. This strongly suggests that the historical pandemic series has a fat tail similar to that of the synthetics. The historical pandemic series tracks the truncated Pareto I complementary cumulative distribution with accuracies comparable to those of the synthetics. The relatively high scatter of the synthetics is due to the small sample size of 72 series elements, corresponding to the historical pandemic series length. Figure A3.1 in Appendix A3 shows the similar plot for synthetics with sample sizes around 1010. There the scatter is reduced significantly.

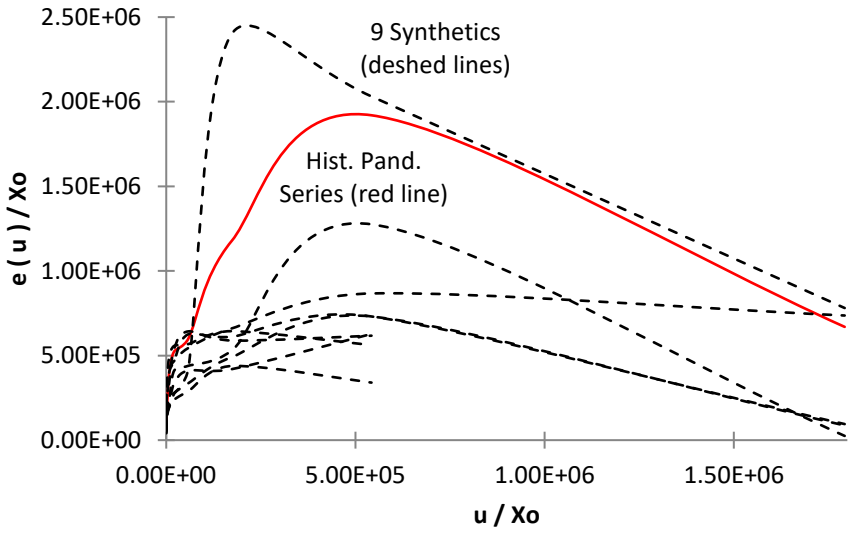

Figure 2.3 Mean excess function's $e(u/x_0)/x_0$ behavior with increasing threshold for the historical pandemic series: historical pandemic results[4] versus the truncated Pareto I synthetics with $\alpha = 0.15$ and $x_{max}/x_0 = 2.7\text{x}10^6$.

Figure 2.3 plots of the mean excess for the nine synthetic power law series (dashed lines) and that of the historical pandemic (red solid line) of equation (2.5). One can see that the paths of the synthetic power-law series envelop the path of the historical pandemic series. Thus the historical pandemic series mimics the behavior of the heavy tailed synthetics. This strongly suggests that the historical pandemic series has a fat tail similar to that of the synthetics. The scatter in the path of the pandemic series is comparable to the scatter in the paths of the synthetics. The relatively high scatter of the synthetics, again, is due to the small sample size of 72. Figure A3.2 in

[4] The plot of the historical mean excess in Figure 2.3 should not be compared to Figure 2c in Cirillo and Taleb (Nature Physics 2020, Figure 4 in the Arxiv.org version) since they plot the average actual numbers (column 5 in their Table 1 multiplied by 1000). Figure 2.3 plots the rescaled ones (their column 7) and is in units of 1000.

Appendix A3 shows that the scatter in the synthetic's tracking of mean excess is greatly reduced for sample sizes around 1110.

Embrechts et. al. (2003, p. 309) describe the plots of ratios of maximum-to-sum as another simple tool to detect heavy tails. To apply this tool, one first forms the sum and maximum of partial empirical series

$$S_m^p = \sum_{k=1}^{m} x_m^p \quad \text{and} \quad M_m^p = \max\,(x_1^p, x_1^p, \cdots, x_m^p). \tag{2.7}$$

In equation (2.7), m ranges between $1 \leq m \leq n$, the series is placed in decreasing rank order of element magnitudes $x_n \leq \cdots x_m \cdots \leq x_1$, and $p = 1, 2, 3, 4$. If the expected value of x^p is finite, $E(x^p) < \infty$, then $M_m^p / S_m^p \to 0$ as $m \to \infty$ (cf. ibid.). One then plots the latter ratios for all m to examine their behaviors. While the pandemic series' ratios, if the distribution is heavy tailed, are not expected to vanish, one never the less gets useful information by comparing the latter's plots of maximum-to-sum ratios to those of the power law synthetic with $\alpha + 1 = 1.15$ (whose ratios do not vanish).

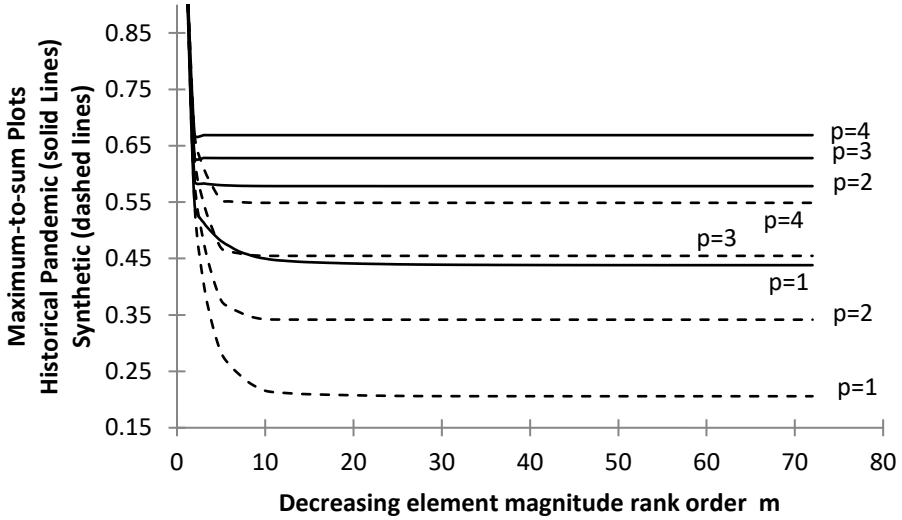

Figure 2.4 Plots of maximum-to-sum ratios' variations with m and p for the historical pandemic series (solid lines) and one of the power-law $1 + \alpha = 1.15$ synthetic series (dashed lines).

Figure 2.4 above shows these ratios for the historical pandemic series (solid lines). It also gives the ratios corresponding to one of the synthetic series (dashed lines). The two plots show that the ratios of maximum to sum behave similarly with increasing m for all values of p. Hence the distribution of historical pandemic series mimics the fat-tailed behavior of the synthetic, and is likely to have a fat tail similar to the synthetics.

3. Comparing Series: Truncated Pareto I to the Worldwide Mortality Rates

Appendix A2 gives the mortality rate series used here with 119 elements. The unit used in this section is $x_0 = 1$. The section uses similar procedures to those presented in Section 2 to study the mortality rate series. It presents the maximum likelihood estimate for this distribution's power law exponent as well as the least-squares-fit estimate of the latter. It finds that the least-squares-fit estimate to be a better representation of the mortality rate series. The section then presents the mean excess above threshold plot for the mortality rate series. It uses the Monte Carlo procedures of Section 2 to generate synthetic power law series. It generates nine sets of such series and compares characteristics of the mortality rate series to those of the synthetics. Zipf plots of the mortality rate series are shown to be very similar to those of the synthetics. The mortality rate series mean excess behavior with increasing thresholds also essentially matches that of the synthetics. These similarities strongly suggest that the mortality rate distribution is likely to be a power law with exponent $\alpha + 1 = 1.45$. Finally, it compares the maximum-to-sum plots of one of the synthetics to that of the mortality rate series. The two plots are quite similar, showing that the mortality rate distribution mimics the behavior of the fat-tailed power law distributions, so its distribution is also likely to be fat tailed.

For the mortality rate series, $x_{max}/x_0 = 125$, α_∞=0.48. This results in $\alpha_{mle} = 0.172$, and the least-squares-fit result is $\alpha_{lsf} = 0.45$.

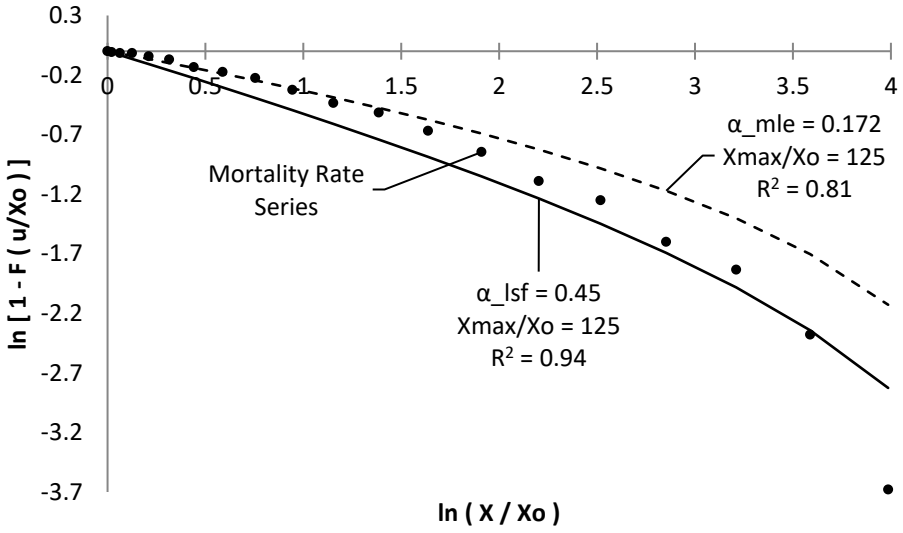

Figure 3.1 Zipf plots of the mortality rate series, and of the truncated Pareto I distributions.

Figure 3.1 above shows the Zipf plot of the mortality rate series (dotted points). The figure also shows the corresponding curves for the truncated Pareto I distributions for α_{mle} (dashed line) and α_{lsf} (solid line) along with their R^2 values of 0.81 and 0.94, respectively. The least-squares-fit is clearly a much better representation of the mortality rate data. The remainder of this section

thus sets $\alpha = \alpha_{lsf} = 0.45$ so that the power law exponent is $1 + \alpha = 1.45$. This section uses this power law to compare the mortality rate series to Monte Carlo synthetic series with equal lengths of 119.

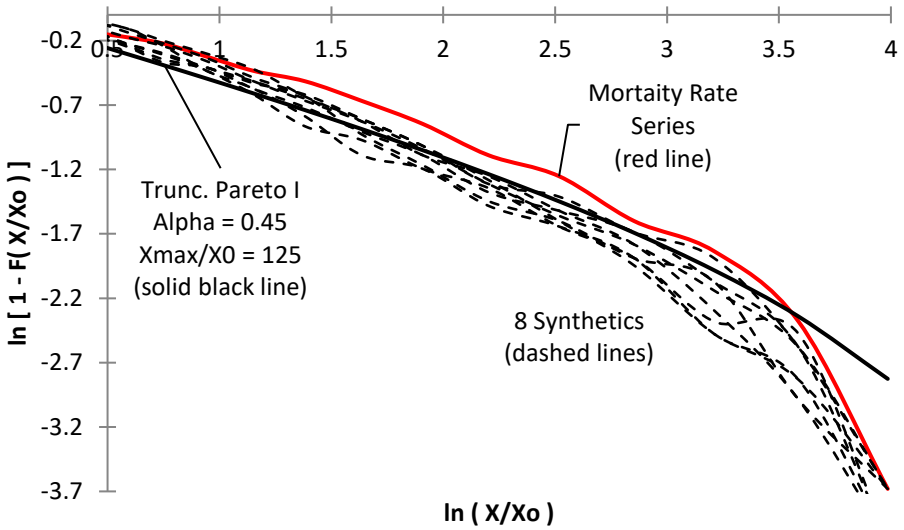

Figure 3.2 shows Zipf plots for the mortality rate series, 8 synthetic series, and of the corresponding truncated Pareto I complementary cumulative distribution.

Figure 3.2 above shows the Zipf plots for the mortality rate series (red solid line), 8 Monte Carlo synthetic series (dashed lines), as well as that of the corresponding truncated Pareto I of equation (2.3). One can see that the paths of the synthetic power-law series essentially envelop the path of the mortality rate series. Thus the mortality rate series mimics the behavior of the heavy tailed synthetics. This strongly suggests that the mortality rate series has a fat tail similar to that of the synthetics. The mortality rate series tracks the truncated Pareto I complementary cumulative distribution with accuracies comparable to those of the synthetics. The relatively high scatter of the synthetics is due to the small sample size of 119 series elements, corresponding to the mortality rate series length. Figure A3.3 in Appendix A3 shows the similar plot for synthetics with sample sizes around 1110. There the scatter is reduced significantly.

Figure 3.3 below plots of the mean excess for the nine synthetic power law series (dashed lines) and that of the mortality rate (red solid line) of equation (2.5). One can see that the paths of the synthetic power-law series envelop the path of the mortality rate series. Hence the mortality rate series mimics the behavior of the heavy tailed synthetics. This strongly suggests that the mortality rate series has a fat tail similar to that of the synthetics. The scatter in the path of the pandemic series is comparable to the scatter in the paths of the synthetics. The relatively high scatter of the synthetics, again, is due to the small sample size of 119. Figure A3.4 in Appendix A3 shows that the scatter in the synthetic's tracking of mean excess is greatly reduced for sample sizes around 1100.

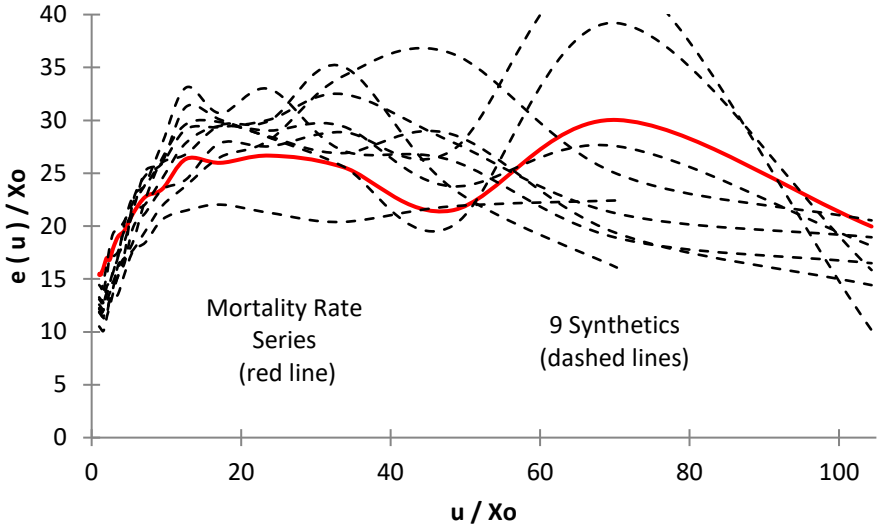

Figure 2.3 Mean excess function's $e(u/x_0)/x_0$ behavior with increasing threshold for the mortality rate series: mortality rate results versus the truncated Pareto I synthetics with $\alpha = 0.45$ and $x_{max}/x_0 = 125$.

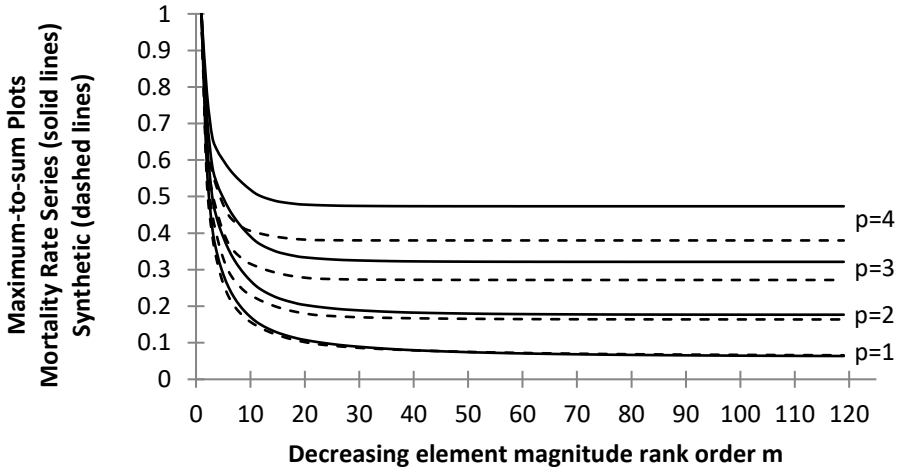

Figure 3.4 Plots of maximum-to-sum ratios' variations with m and p for the mortality rate series (solid lines) and one of the power-law $1 + \alpha = 1.45$ synthetic series (dashed lines).

Let's now consider the maximum-to-sum plots obtained from equations (2.7) for the mortality rate series. Figure 3.4 above shows these ratios for the mortality rate series (solid lines). It also gives the ones corresponding to one of the synthetic series (dashed lines). The two plots show that the ratios of maximum to sum behave similarly with increasing m for all values of p. Hence

the distribution of mortality rate series mimics the fat-tailed behavior of the synthetic, and is likely to have a fat tail too.

4. Summary and Discussion

Section 2 studied the historical pandemic series using methods of extreme value theory. It used a least-squares-fit estimate for the truncated Pareto I distribution to determine the specific historical pandemic power law exponent $\alpha + 1 = 1.15$. It then compared the behaviors of several Monte Carlo synthetic series with this power law to the historic pandemic series, producing the following results. The Zipf plots showed very similar behaviors. The mean excess behavior of the historical pandemic series mimics those of the synthetics, with all excesses initially increasing with thresholds. Plots of the ratio of maximums-to-sums showed very similar trends. The harmony in behaviors between the pandemic series and synthetic ones in all of the above ways strongly suggests that the historical pandemic series has a fat tail similar to that of the synthetics.

Section 3 studied the worldwide mortality rates using the procedures of Section 2. It used a least-squares-fit estimate of the truncated Pareto I distribution to determine the specific mortality rate power law exponent $\alpha + 1 = 1.45$. It then compared the behaviors of several Monte Carlo synthetic series with this power law to the mortality rate series, producing the following results. The Zipf plots showed very similar behaviors. The mean excess behavior of the mortality rate series mimics those of the synthetics, with all excesses initially increasing with thresholds. Plots of the ratio of maximums-to-sums showed very similar trends. The harmony in behaviors between the mortality rate series and synthetic ones in all of the above ways strongly suggests that that the mortality rate series has a fat tail similar to that of the synthetic series.

The historical pandemic distribution is predominately determined by ancient history. Sixty-one of its epidemics' endings predate the twenty-first century. All of the more recent plagues have also died out, except for Covid-19. In this sense, it is an unchanging distribution fixed in stone. The mortality rate distribution, on the other hand, is less than a year old. It is currently evolving as the various worldwide countries respond differently to their local respective epidemics.

The tail index $\alpha + 1 = 1.15$ of the historical pandemic series is significantly smaller than that of the current mortality rate series $\alpha + 1 = 1.48$. This indicates that the historical pandemic distribution's behavior is wilder than that of the current mortality rate series. Let us consider possible reasons for this. Clearly medical care has improved significantly over the ages, resulting in a reduction in pandemic-related fatalities. Further, communications are much faster now than in the past, permitting quicker spread of pandemic danger alerts and more rapid roll out of preventive lockdown measures. Countering these positive pandemic control factors are the current much faster and more extensive travel by air that aids the spread of the coronavirus.

Another stumbling block that promotes viral transmission is the public aversion to strong lockdown measures due to the harsh economic consequences resulting from the latter. Considering the sum of these factors, one might speculate that the current mortality distribution has a milder behavior than that of the historical pandemics because the first two positive factors win out over the last two negative ones. On the other hand, one could also guess that because the Covid-19 pandemic is not even one year old, its behavior may get much wilder as it matures, matching the savagery of the historical pandemic. The future's unfolding will reveal the path the present pandemic follows.

The evolution of the worldwide pandemic mortality rate exponent depends on how much coordination occurs between the countries. If many countries take parallel and persistent (versus chaotic and weak) responses to the epidemic, the mortality rate distribution will change: the current fat-tailed distribution may swerve in the future toward milder (versus wilder) fat-tail behavior, having higher (versus lower) power laws.

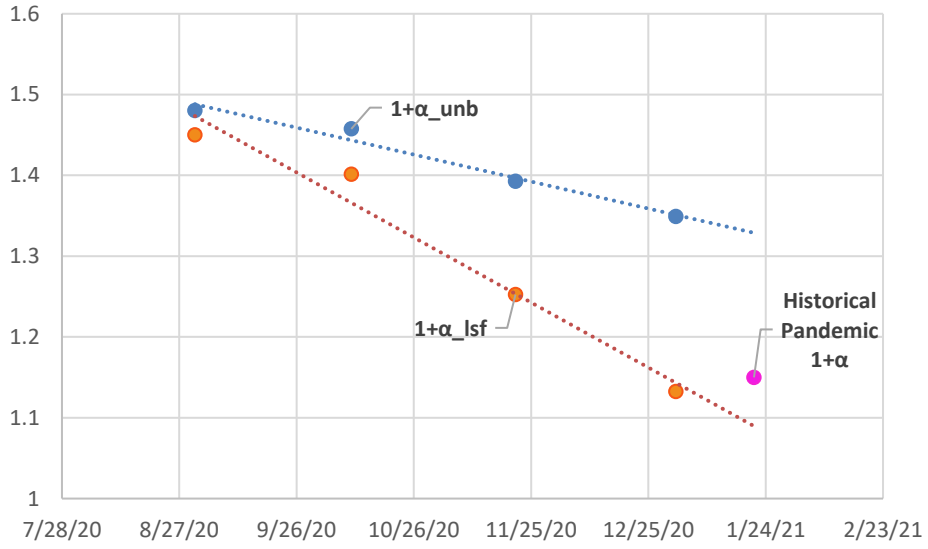

Figure 4.1 Recent readings of the mortality rate exponents and their trends.

Table 4.1 Values of the mortality rate's power law exponents for several recent dates.

Date	8/31/20	10/10/20	11/21/20	1/1/21
$1+\alpha_{unb}$	1.480	1.457	1.393	1.349
$1+\alpha_{lsf}$	1.450	1.401	1.253	1.133
x_{max}/x_0	125	125	139	143

Forebodingly, over the past several months the worldwide mortality rate's exponent has been trending steadily downward. This exponent was determined on recent dates as shown in Table

4.1 above for both the unbounded ($1+\alpha_{unb}$) and the least-square-fit truncated Pareto I distributions. The cut-offs for the latter distributions are also given in the table.

Figure 4.1 above plots these readings and the trend lines they project. One can see that the least-square-fit exponent has already decreased below the value of the historic pandemic one. For the unbounded case, if the trend maintains its pace, the mortality rate's exponent will approach the historical pandemic's lower value by the middle of July, 2021.

Sections 2 and 3 used the truncated Pareto I distribution. This was due to the limited data available, i.e., the historical pandemic series and the mortality rate series as of August 31, 2020. One does not know how high the pandemic death toll will climb[5], and the remainder of this section assumes the unbounded distribution.

The mortality rate distribution may also be altered by an individual country's determined and sustained (versus lackadaisical and failing) response, which may shift its position in future pandemics distributions to less (versus more) catastrophic regions.

Table 4.2 Top eleven countries in decreasing rank order of mortality rate magnitudes and the status of their virus response.

Rank Order	Country	Status of Virus Response
1	San Marino	Beating virus
2	Peru	Needs to take action
3	Belgium	Needs to take action
4	Andorra	Beating virus
5	United Kingdom	Needs to take action
6	Spain	Needs to take action
7	Chile	Needs to take action
8	Italy	Needs to take action
9	Brazil	Needs to take action
10	Sweden	Nearly there
11	United States	Needs to take action

Let's look at the recent efforts against the pandemics by countries within the top eleven mortality rates. Table 4.2 shows these countries in decreasing rank order of mortality rate magnitudes, along with the status[6] of each country's virus response to its epidemic. This status varies from "Needs to take action," to "Nearly there," to "Beating virus." Note that San Marino and Andorra

[5] The only certain upper bound to the death toll is the entire world population, which from a practical point of view is infinite.

[6] Statuses of countries' efforts against the virus are from the EndCoronavirus.org web site, at: https://www.endcoronavirus.org/countries#nearly .

are now beating the virus although they rank first and fourth in mortality rate magnitudes, respectively. Assuming that their virus responses maintain their good status into the far future, their mortality rate magnitudes will presumably drop, while other countries with weaker efforts will see increases. Sweden is nearly there, so three out of eleven countries may be destined for an optimistic outcome. This gives an admittedly sketchy probability of rosy outcomes for an average country at the highest mortality rates of about 27%.

Table 4.3 Twenty-three countries in the total mortality rate series with mortality rates above unity that are beating the coronavirus currently, or are nearly there.

Rank Order	Country	Mortality Rate	Rank Order	Country	Mortality Rate
1	San Marino	124.32	74	Estonia	4.85
4	Andorra	68.83	81	Mauritania	3.61
23	Kosovo	26.45	84	Belize	3.39
26	South Africa	24.49	91	Pakistan	2.97
35	Kyrgyzstan	16.75	95	Australia	2.63
44	Saudi Arabia	11.56	99	Barbados	2.44
46	El Salvador	11.17	102	Sudan	1.97
50	Serbia	10.21	106	Latvia	1.76
54	Kazakhstan	8.33	108	Cyprus	1.68
61	Qatar	7.08	110	Cameroon	1.63
65	Djibouti	6.26	118	Kenya	1.12
68	Egypt	5.51			

One doesn't know if these countries can maintain their successful efforts in the future, so let's describe them as countries in epidemic remission. In the discussion below, this term will be applied to all countries with a virus response status of "beating virus", or "nearly there".

Table 4.3 above shows the twenty-three countries that are in epidemic remission from the data set used here with 119 countries. This table also shows their rank in mortality rate magnitude and their mortality rate. Here, the probability of the optimistic outcome of epidemic remission is lowered to 23 out of 119 countries, or 19% for countries with mortality rates above unity.

Note that the countries in epidemic remission have mortality rate magnitudes ranging from nearly the lowest one to the highest one. This suggests that a country's current mortality rate has no bearing on its achievement of epidemic remission. Hence, a country's path to epidemic remission appears not to be tethered to the unstable and dangerous mortality rate power law distribution. Furthermore, three countries with the top ten highest mortality rate magnitudes have achieved epidemic remission, as noted above. This suggests that while a county's past determines its position on the ranked power law sequence, it's likely the strength of its response

to the epidemic that determines its future, not the mortality power law distribution[7]. The pandemic's progression should either support or negate these premises.

The Pareto I distributions discussed here allow extreme catastrophic events to occur frequently. Thus, both the historical pandemic and current mortality rate evidence demands extreme caution when dealing with epidemics. Let us now consider the predictive capabilities of power law distributions. A possible approach is through the value-at-risk concept used in finance. For power law distributions, the value at risk can be expressed analytically (cf. Neslehova, Embrechts, and Chavez-Demoulin, 2006, p. 5), and is given by $VaR_{1-\varepsilon} = x_0\varepsilon^{-\frac{1}{\gamma}}$, where γ is the power law exponent. This value at risk means that in $1/\varepsilon$ trials one result will likely exceed the value of $x_0\varepsilon^{-\frac{1}{\gamma}}$. In financial practice, $1-\varepsilon$ is expressed as a percentage and typically $\varepsilon = 0.1\%$. For the historical pandemic series with $\gamma = \alpha + 1 = 1.15$ and $x_0 = 10^3$, one obtains $VaR_{99.9\%} =$ 399,000. This means that 1 in a1000 times the fatalities will likely exceed 399,000 deaths. While this statement is mathematically precise, it's illusory for the following reason. One must also consider the average of the fatalities above the value-at-risk threshold of 399,000 deaths. For the pandemic distribution, $\alpha = .15$ so the Pareto I distribution's average above the given threshold is infinite[8]. The latter result holds for all $\varepsilon > 0$. This renders the value-at-risk premise "in $1/\varepsilon$ trials, one result will probably exceed…" a meaningless non sequitur: for any and all trial sets $1/\varepsilon$, the mean of the deaths above each set's respective thresholds $x_0\varepsilon^{-\frac{1}{\gamma}}$ is crushingly huge[9] (infinite). Thus, while their fat tails red-light dangers that power law distributions pose, these distributions cannot provide specific predictions on or even ranges for devastating events to guide pandemic responses.

Clearly the evolution of the mortality rate distribution will depend on myriads of unknown factors in the individual responses of each of the worldwide countries. Given the wide chasm of uncertainty faced by each country against this coronavirus, epidemic forecasts may provide useful guidance in the efforts against the virus -- if the forecasts can be made more reliable, as championed by Ioannidis et.al. (2020). Projections like those presented[10] by the Institute for Health Metrics and Evaluation at the University of Washington are instructive and motivational. They project out to April 2021 for current best estimates of the United States response to the coronavirus. They also give a projection that includes the effects of easing of mandates, and one

[7] Tables 4.2 and 4.3 were completed around the end of September, 2020. Some of the statuses of the countries' virus responses or mortality rankings have changed. However, the points noted in this paragraph still remain relevant.

[8] For the Pareto I distribution, this average is given by $\frac{\int_{\frac{u_\varepsilon}{x_0}}^{\infty} xf(x)dx}{\int_{\frac{u_\varepsilon}{x_0}}^{\infty} f(x)dx} = \begin{cases} \infty & for\ \ \alpha \le 1 \\ \frac{\alpha}{\alpha-1}\frac{u_\varepsilon}{x_0} & for\ \ \alpha > 1 \end{cases}$, where $u_\varepsilon = x_0\varepsilon^{-\frac{1}{\gamma}}$.

[9] Heedless individuals might be enticed by the "one chance in $1/\varepsilon$ trials" with ε below 10^{-3}, being wittingly or unwittingly blind to likely realizations of crushingly huge fatalities. Such an approach does not give a useful epidemic projection- instead- it misleadingly presents lower devastation magnitudes than those likely to occur.

[10] Available at: https://covid19.healthdata.org/global?view=total-deaths&tab=trend .

that includes effects of universal mask use. Their current best estimate for total deaths by April is about 567,000. Universal mask use would lower the fatalities to about 518,000, while easing of mandates increases the death toll to about 731,000. The large differences in death tolls should encourage rational individuals to wear masks and support gradual, not hasty, easing of mandates.

Finally, this discussion ends by summarizing the results in Appendix 1. This appendix determines the maximum likelihood parameters for two possible Gamma function representations of the historical pandemic data. Using Monte Carlo methods, it generates several sets of Gamma-function-distributed series with the same length as the pandemic one. It then looks at typical events that each Gamma distribution generates. It finds that the scales of each Gamma distribution's typical events are orders of magnitudes smaller than the scale of the historical epidemics. Hence, the Gamma distributions are not relevant to studies of the historical pandemic series.

The author thanks Damon Larson for editing parts of this manuscript.

Appendix 1 Comparing Gamma Distributions to the Pandemic Series

This section determines the maximum likelihood parameters of two Gamma distributions: 1) one where the pandemic series' elements are the Gamma function's arguments and 2) one where the logarithms of the series' elements are its arguments. It then generates several sets of Gamma function deviates each containing the same number of elements as the historical pandemic series for each Gamma function representation. It then looks at typical events that the two Gamma distributions generate. It finds that the scales of these typical events are orders of magnitudes smaller than the scale of the historical epidemics. Hence the Gamma distribution representations are not relevant to studies of the historical pandemic series.

This appendix uses the variable $y = x/x_0$, where $x_0 = 1000$. The two Gamma distributions with shape α and scale β parameters are

$$f(y,\alpha,\beta) = \frac{y^{\alpha-1}}{\Gamma(a)\beta^a} e^{-\frac{y}{\beta}}, \quad \text{and} \quad f(lny,\alpha,\beta) = \frac{(ln\, y)^{\alpha-1}}{\Gamma(a)\beta^a} e^{-\frac{lny}{\beta}}. \tag{A1.1}$$

The rightmost distribution was posited as a possible fit to the pandemic data by Ioannidis et.al. (2020). Let us first consider the leftmost distribution.

The equations that the maximum likelihood parameters satisfy are straight forwardly determined[11] and are given by

$$\beta = \langle y_i \rangle/\alpha \tag{A1.2}$$

[11] For example, see the Wikipedia page at https://en.wikipedia.org/wiki/Gamma_distribution.

$$\langle \ln y_i \rangle - \frac{\Gamma'(\alpha)}{\Gamma(\alpha)} - \ln \langle y_i \rangle + \ln \alpha = 0. \quad \text{(A1.3)}$$

In the above equations, the angle brackets denote pandemic series averages, $\Gamma(\alpha)$ is the Gamma function, and $\Gamma'(\alpha)$ is its first derivative.

Table A1.1 Maximum likelihood Gamma function parameters for the historical pandemic series

$f(x, \alpha, \beta)$				
$Arguement\ x$	α	β	$\mu = \alpha\beta$	$\sigma = \sqrt{\alpha\beta^2}$
y	0.159	5.34×10^5	8.49×10^4	2.13×10^5
$ln\ y$	2.60	0.643	1.67	1.04

The approximation $\Gamma'(\alpha) = [\Gamma(\alpha + .001) - \Gamma(\alpha - 0.001)]/0.002$ was used to solve Equation (A1.3). The resulting maximum likelihood Gamma function parameters are given in the first numerical row of the Table A1.1 above, along with the distribution's mean μ and standard deviation σ.

Liu, C., Martin, R., Syring, N. (2015) give a procedure for generating this Gamma distribution's deviates. The author implemented their procedure to generate 10,000 deviates. This set of deviates reproduced the mean and standard deviation in table A1.1 with accuracies better than 0.5%.

Now consider the rightmost distribution in equation (A1.1). The equations that the maximum likelihood parameters satisfy for this logarithmic representation are obtained by substituting $y_i \rightarrow ln\ y_i$ into equations (A1.2) and (A1.3):

$$\beta = \langle ln\ y_i \rangle / a \quad \text{(A1.4)}$$

$$\langle \ln (ln\ y_i) \rangle - \frac{\Gamma'(\alpha)}{\Gamma(\alpha)} - \ln (\langle ln\ y_i \rangle) + ln\alpha = 0. \quad \text{(A1.5)}$$

The solutions to these equations are given in the second numerical row of Table A1.1, along with this distribution's mean and standard deviation.

The Wikipedia page[12] on Gamma distributions summarizes Marsaglia's procedure for generating deviates of this distribution. The author implemented this procedure to generate 10,000 deviates. This set of deviates reproduced the mean and standard deviation in Table A1.1 with accuracies of 0.5%.

The above procedure for producing synthetic deviates of the Gamma representation $f(y, \alpha, \beta)$ of the epidemic series was used to generate nine sets of series having lengths of 72, equal to that of the historical pandemic one. The summary parameters $max(x_i)$, mean $\mu = \langle x_m \rangle$, and standard

[12] Available at: https://en.wikipedia.org/wiki/Gamma_distribution.

deviation σ_{x_m} were computed for each set, giving ranges for each one over the nine sets. Table A1.2 below gives the results along with the corresponding parameters of the Gamma function representation. One can see that the most common series described by this Gamma representation have much smaller maximum elements, much lower series' element means, and much more restricted deviations around their means. Hence a typical event described by this Gamma representation is on a much smaller scale than that of the pandemic series by factors over 500 for each of the summary parameters. Thus this Gamma representation is not relevant to studies of the historical pandemic series.

Table A1.3 below shows the results of the above procedure applied to generate typical series of the Gamma representation[13] $f(lny, \alpha, \beta)$. One again sees that all of the summary parameters of the historical pandemic series vastly exceed the ranges of typical series described by this Gamma representation, and thus the latter is not relevant to studies of the historical pandemic series.

Table A1.4 below shows the results of the above procedure when applied to the truncated Pareto I distribution $f(x/x_0)$ corresponding to the historical epidemic series $1 + \alpha = 1.15$. One can see that the Pareto I distribution's typical series have summary parameter ranges that accommodate the historical pandemic's summary parameters. Hence it can be appropriately used to study the historical pandemic distribution.

[13] In this case one first determines the respective summary parameter's logarithms and then takes their exponential value.

Table A1.2 Nine Gamma functions $f(y, \alpha, \beta)$ series' summary parameters compared to those of the historical pandemic.

$f(y, \alpha, \beta)$										Range:		Historical
Series # =	1	2	3	4	5	6	7	8	9	Min	Max	Pandemic
$Max(x_m)$	1.2E+03	2.1E+03	1.4E+03	1.5E+03	1.2E+03	2.2E+03	1.2E+03	1.4E+03	8.4E+02	8.4E+02	2.2E+03	2.7E+06
$\mu = \langle x_m \rangle$	1.4E+02	1.8E+02	1.8E+02	1.5E+02	1.0E+02	2.6E+02	1.1E+02	1.6E+02	1.3E+02	1.0E+02	2.6E+02	8.5E+04
σ_{x_m}	2.1E+02	3.3E+02	3.0E+02	2.5E+02	1.9E+02	4.0E+02	2.0E+02	2.5E+02	2.0E+02	1.9E+02	4.0E+02	4.1E+05

Table A1.3 Nine Gamma functions $f(lnx, \alpha, \beta)$ series' summary parameters compared to those of the historical pandemic.

$f(lny, \alpha, \beta)$										Range:		Historical
Series # =	1	2	3	4	5	6	7	8	9	Min	Max	Pandemic
$Max(x_m)$	1.1E+02	3.7E+02	1.0E+03	2.3E+04	1.7E+02	4.4E+02	1.4E+02	1.5E+04	1.9E+02	1.1E+02	2.3E+04	2.7E+06
$\mu = \langle x_m \rangle$	1.4E+01	1.4E+01	1.9E+01	2.2E+01	1.3E+01	1.4E+01	1.4E+01	1.5E+01	2.0E+01	1.3E+01	2.2E+01	8.5E+04
σ_{x_m}	2.4E+00	2.5E+00	3.1E+00	4.9E+00	2.1E+00	2.4E+00	2.3E+00	3.5E+00	2.6E+00	2.1E+00	4.9E+00	4.1E+05

Table A1.4 Nine Pareto I distribution series' summary parameters compared to those of the historical pandemic.

$Pareto\ I$ $f(x/x_0)$										Range:		Historical
Series # =	1	2	3	4	5	6	7	8	9	Min	Max	Pandemic
$Max(x_m)$	1.9E+06	3.0E+06	2.3E+06	2.9E+06	2.6E+06	2.7E+06	2.7E+06	2.8E+06	1.8E+06	1.8E+06	3.0E+06	2.7E+06
$\mu = \langle x_m \rangle$	9.5E+04	1.1E+05	8.5E+04	7.5E+04	1.7E+05	1.0E+05	1.1E+05	6.2E+04	8.1E+04	6.2E+04	1.7E+05	8.5E+04
σ_{x_m}	3.8E+05	4.5E+05	3.3E+05	3.8E+05	4.9E+05	3.9E+05	4.5E+05	3.4E+05	3.3E+05	3.3E+05	4.9E+05	4.1E+05

Appendix A2 Mortality Rate Series Data

On 8/31/20 the worldwide mortality rates (deaths/100K population) were copied from the Johns Hopkins Coronavirus Resource Center's web site[14]. Mortality rates smaller than 1, were discarded. Table A2.1 below gives the elements of the mortality rate series with 119 elements.

Table A2.1 Worldwide mortality rates (deaths/100K population).

Rank	Mortality Rate	Rank	Mortality Rate	Rank	Mortality Rate	Rank	Mortality Rate
1	124.32	31	18.59	61	7.08	91	2.97
2	89.99	32	18.32	62	6.43	92	2.83
3	86.63	33	18.32	63	6.34	93	2.77
4	68.83	34	17.72	64	6.3	94	2.65
5	62.55	35	16.75	65	6.26	95	2.63
6	62.27	36	16.09	66	6.09	96	2.5
7	60.27	37	16.07	67	5.84	97	2.48
8	58.72	38	16	68	5.51	98	2.48
9	57.95	39	14.18	69	5.43	99	2.44
10	57.04	40	12.83	70	5.37	100	2.44
11	56.12	41	12.33	71	5.37	101	2.12
12	51.04	42	12.11	72	5.01	102	1.97
13	47.93	43	11.86	73	4.97	103	1.81
14	45.74	44	11.56	74	4.85	104	1.81
15	44.28	45	11.22	75	4.83	105	1.79
16	39.6	46	11.17	76	4.69	106	1.76
17	38.37	47	10.76	77	4.55	107	1.7
18	36.61	48	10.57	78	3.99	108	1.68
19	36.28	49	10.34	79	3.99	109	1.66
20	29.78	50	10.21	80	3.77	110	1.63
21	28.95	51	9.91	81	3.61	111	1.58
22	28.06	52	8.95	82	3.58	112	1.49
23	26.45	53	8.72	83	3.55	113	1.47
24	26.37	54	8.33	84	3.39	114	1.4
25	24.75	55	8.29	85	3.34	115	1.34
26	24.49	56	8.01	86	3.33	116	1.33
27	23.55	57	7.74	87	3.17	117	1.28
28	20.4	58	7.36	88	3.12	118	1.12
29	19.54	59	7.18	89	3.08	119	1.03
30	19.46	60	7.11	90	3.06		

[14] Available at: https://coronavirus.jhu.edu/data/mortality. Note current individual elements in this rank ordered table may differ from those in Table A2.1 which was copied from the web site last August.

Appendix A3 Comparing Big Sample-Size Synthetics to Expected Behaviors

This appendix presents charts comparing the behaviors of larger sample size synthetics to their expected tracks. Each figure presented below corresponds to a figure in either Section 2 (with sample size of 72) or Section 3 (with sample size of 119). These charts are presented to demonstrate that the large scatter in the corresponding figures presented in these Sections is due to their small sample sizes. The figures with sample sizes noted on them along with their captions are self-explanatory, so that no additional comments accompany them.

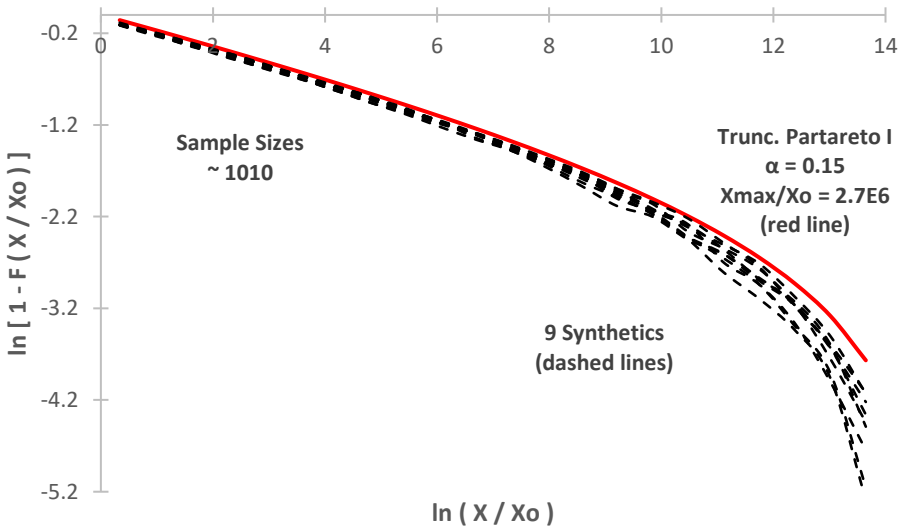

Figure A3.1 Zipf plots for the synthetic series and the truncated Pareto I complementary cumulative distribution corresponding to the historical pandemic series.

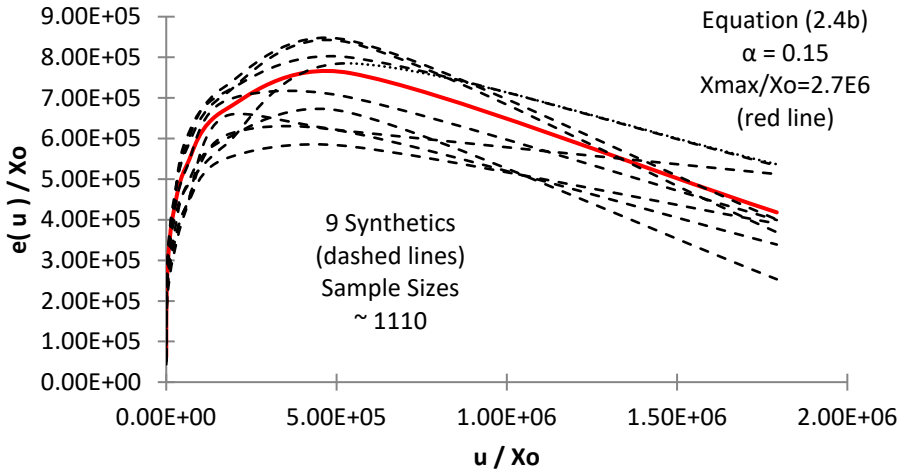

Figure A3.2 Mass excess $e(u)/x_0$ behaviors with increasing threshold for parameters corresponding to the historical pandemic series.

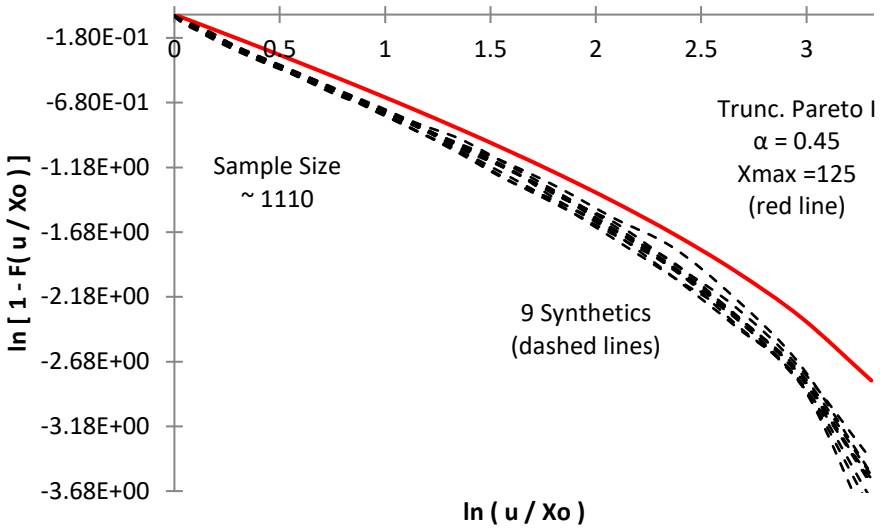

Figure A3.3 Zipf plots for the synthetic series and truncated Pareto I complementary cumulative distribution corresponding to the mortality rate series.

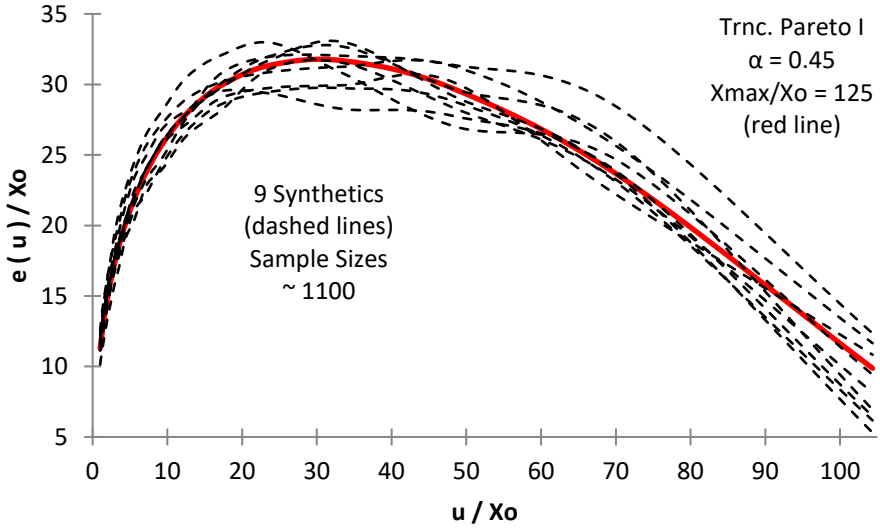

Figure A3.4 Mass excess $e(u)/x_0$ behaviors with increasing threshold for parameters corresponding to the mortality rate series.

References

Aban, I. B., Meerschaert, M. M., Panorska, A. K., (2006) Parameter Estimation for the Truncated Pareto Distribution, Journal of the American Statistical Association, Vol. 101, No. 473, pp. 270-277. Available at: https://www.stt.msu.edu/~mcubed/TPareto.pdf .

Cirillo, P. (2013) Are Your Data Really Pareto Distributed? Physica A: Statistical Mechanics and its Applications 392, 5947-5962. Available at: https://arxiv.org/pdf/1306.0100.pdf .

Cirillo, P. and Taleb N.N. (2020) Tail Risk of Contagious Diseases, Nature Physics 16, pp. 606-613. Available at: https://www.nature.com/articles/s41567-020-0921-x.

Clauset A., Shalizi C.R., and Newman M.E.J. (2009) Power-law Distributions in Empirical Data, SIAM Review 51, pp. 661-703. Available at: https://arxiv.org/pdf/0706.1062.pdf.

Embrechts, P., Klüppelberg, C., and Mikosch, T. (2003) Modelling Extremal Events, (Springer). Available at: http://web.math.ku.dk/~mogens/springerchap6.pdf.

Liu, C., Martin, R., and Syring, N. (2015) Simulating from a Gamma Distribution with Small Shape Parameter, Available at: https://arxiv.org/pdf/1302.1884.pdf.

Ioannidis J.P.A., Cripps S., Tanner M.A. (2020). Forecasting for COVID-19 Has Failed. International Institute of Forecasters, Available at: https://forecasters.org/blog/2020/06/14/forecasting-for-covid-19-has-failed/.

Neslehova, J., Embrechts, P., and Chavez-Demoulin, V. (2006) Infinite Mean Models and the LDA for Operational Risk, Available at: https://people.math.ethz.ch/~embrecht/ftp/manuscript.pdf .

Press, W. H., Flannery, B. P., and Teukolsky, W. T. (2002) Numerical Recipes in C++: the Art of Scientific Computing, (Cambridge University Press).
Available at: https://www.cec.uchile.cl/cinetica/pcordero/MC_libros/NumericalRecipesinC.pdf

Taleb N. N., Bar-Yam Y., and Cirillo P. (2029) On Single Point Forecasts for Fat-tailed Variables, International Journal of Forecasting. Available at: https://arxiv.org/pdf/2007.16096.pdf.